HHS Public Access

Author manuscript

Pain. Author manuscript; available in PMC 2019 September 01.

Published in final edited form as:

Pain. 2018 September ; 159(9): 1719–1730. doi:10.1097/j.pain.0000000000001258.

NALCN channels enhance the intrinsic excitability of spinal projection neurons

Neil C. Ford, M.S.,
University of Cincinnati College of Medicine

Dejian Ren, Ph.D, and
University of Pennsylvania

Mark L. Baccei, Ph.D
University of Cincinnati College of Medicine

1. Introduction

Approximately 80% of lamina I projection neurons in the spinal superficial dorsal horn (SDH) innervate the parabrachial nucleus (PBN), contributing to a larger ascending pathway through which nociceptive signals detected in the periphery reach the brain [30,80]. Spino-parabrachial (PB) neurons respond to noxious stimuli from the first days of life [56], suggesting that this pathway is instrumental for pain sensation in both children and adults. PBN activation by spino-PB input contributes to the emotional valence of pain perception through its connections with the amygdala and drives descending inhibition via rostral ventromedial medulla (RVM) activation [10,20,33,73]. Despite the clear importance of spino-PB neurons for pain processing, relatively little is known about the factors which regulate the intrinsic membrane excitability of this key neuronal population, particularly during early postnatal development. As a result, the underlying ionic mechanisms that shape the flow of nociceptive information from the immature spinal cord to the brain are still unclear.

Our recent work demonstrated that voltage-independent (i.e. “leak”) inward-rectifying K^+ ($K_{ir}2$) channels strongly dampen membrane excitability within neonatal spino-PB neurons [19]. Nonetheless, the complement of leak ion channels expressed in developing projection neurons, particularly those which may constitutively enhance neuronal excitability, remain poorly understood. The non-selective Na^+ leak channel NALCN [43] facilitates the firing of neurons in the brain [50,74], and NALCN mRNA is widely expressed in the spinal cord [50]. Unfortunately, the degree to which NALCN channels shape the excitability of spinal projection neurons has yet to be explored at any stage of postnatal development.

The firing of spinal projection neurons is strongly controlled by neuromodulators released from primary afferent C-fibers, including but not limited to substance P (SP) [8,9,21,66,72]. The majority (~80%) of lamina I projection neurons express the SP receptor NK1R [56,81],

Correspondence to: Neil C. Ford, M.S., Graduate Assistant, University of Cincinnati College of Medicine, Anesthesiology, 231 Albert Sabin Way, 1864 CARE/Crawley, Cincinnati, OH 45267, UNITED STATES, +1-513-558-1309, fordnc@mail.uc.edu.

which evokes a slow membrane depolarization in dorsal horn neurons [13,31,48,81] via multiple downstream mechanisms including the closure of G protein-coupled K^+ (GIRK) channels [42,64,76,79]. Interestingly, SP has been shown to activate a NALCN-mediated conductance in the brain [51]. This raises the intriguing, but as yet untested, possibility that the effects of SP release on spinal nociceptive processing are mediated in part via actions on NALCN channels expressed within SDH neurons. Given that NK1R-expressing projection neurons are thought to be essential for mechanical and thermal hyperalgesia under pathological conditions [56,59,68], it is important to fully understand the mechanisms by which SP regulates action potential discharge in this population.

The present study identifies NALCN channels as both potent regulators of activity within spinal projection neurons and key targets of SP signaling within the spinal nociceptive network. Collectively, these results add new insight into the ionic mechanisms that govern the level of ascending nociceptive transmission to the developing brain, and may therefore have important implications for the neurobiological underpinnings of pediatric pain.

2. Materials and Methods

All animal experiments were conducted with strict adherence to the animal welfare guidelines set forth by the University of Cincinnati Institutional Animal Care and Use Committee.

2.1 Retrograde labeling of spino-parabrachial neurons in neonatal rats

On postnatal day 1 (P1), male and female Sprague-Dawley rats were anesthetized with an intraperitoneal (I.P.) injection of a 10 : 1 mixture of ketamine (90 mg / kg) and xylazine (10 mg / kg), then secured to a custom plaster mold mounted to a stereotaxic frame (World Precision Instruments, Inc. Sarasota, FL, USA). Under sterile conditions, lambda as well as parts of the parietal and occipital bones were exposed by surgical incision. Using a drill (OmniDrill-35; World Precision Instruments, Inc. Sarasota, FL, USA) fitted with a ball mill carbide # ¼ burr (World Precision Instruments, Inc.), a hole was made above the right PBN at stereotaxic coordinates (in mm, with respect to lambda): - 2.7 rostrocaudal (RC), - 1.0 mediolateral (ML), - 4.3 dorsoventral (DV). FAST DiI oil (2.5 mg / ml) was loaded into a Hamilton microsyringe (62RN; 2.5 μl) fitted with a 28-gauge needle, which was then placed into a microsyringe injector (Micro-4; World Precision Instruments, Inc.). The needle was positioned in the PBN, and 120 nl of DiI was injected at a rate of 25 nl / min. After the injection, the needle position was maintained for at least 1 minute to allow for optimal DiI delivery. The needle was carefully withdrawn, and the surgical wound was closed using Vetbond (3M, St. Paul, MN, USA). Animals were then placed on an electric heat pad maintained at 37 °C, under close observation, until recovery from anesthesia. Animals were then returned to their home cage for 2–4 days prior to the initiation of the electrophysiological studies.

2.2 Cre-dependent NALCN knockout in mouse spino-parabrachial neurons

P3 C57BL6 mice, containing loxP sites inserted to flank NALCN protein coding regions ($NALCN^{f/f}$; [86]), of both sexes were anesthetized by I.P. injection of a 10 : 1 mixture of

ketamine (90 mg / kg) and xylazine (2 mg / kg). Mice were then secured in a custom 3-D printed mold (Desktop MakerBot Replicator+ 5th generation; MakerBot Industries, LLC., Brooklyn, NY, USA) and secured to a stereotaxic frame (World Precision Instruments, Inc.). Under sterile conditions, using a 30-gauge needle, a hole was made through the skin and occipital bone over the right PBN at stereotaxic coordinates (in mm, with respect to lambda): - 1.9 RC, - 1.0 ML, -3.0 DV. AAV1.hSyn.eGFP.WPRE.bGH (GFP; Titer: 3.86 x 10^{13} genome copies (GC) / ml) or AAV1.hSyn.HI.eGFP-Cre.WPRE.SV40 (Cre; Titer: 9.2 x 10^{12} GC / ml; University of Pennsylvania Center for Molecular Therapy of Cystic Fibrosis Vector Core) was loaded into a Hamilton microsyringe (62RN; 2.5 μl) fitted with a 33-gauge needle, which was then placed into a microsyringe injector (Micro-4; World Precision Instruments, Inc.). 200 nl of viral stock was injected into the PBN at a rate of 25 nl / min. After completion of the injection, the needle was left in place for at least 2 minutes to allow for maximal virus delivery before it was carefully removed from the injection site. The animals were then placed under close observation on an electric heating pad set at 37 °C until full recovery from anesthesia. Animals were returned to their home cage where they remained for 7–10 days before electrophysiological experiments to allow for full retrograde transport and to ensure maximal infection and Cre / GFP expression in spino-PB neurons. Identification of virus-infected spino-PB neurons was facilitated by the expression of cytoplasmic GFP by AAV1-hSyn-eGFP or GFP-tagged Cre by AAV1-hSyn-eGFP·Cre.

2.3 In vitro intact spinal cord and slice preparations

Tissue preparation was performed as previously reported [19,44], and briefly described below. P3–5 DiI-injected rat pups, or P10–14 AAV-infected mouse pups, were deeply anesthetized with an I.P. injection of sodium pentobarbital (30 mg / kg; Fatal-Plus, Vortec Pharmaceuticals, Dearborn, MI, USA). Animals were then transcardially perfused with ~ 5–10 ml of oxygenated (95% O_2 / 5% CO_2) dissection solution composed of (in mM): 250 sucrose, 2.5 KCl, 25 $NaHCO_3$, 1 NaH_2PO_4, 25 glucose, 6 $MgCl_2$, 0.5 $CaCl_2$, 25 glucose (pH = 7.2). The vertebral column was carefully isolated then placed in a dissection chamber with dissection solution under constant oxygenation.

For the intact spinal cord preparation in rats and mice, the spinal cords were dissected out of the vertebral column then stripped of all meninges before blocking the tissue around the lumbar enlargement. For the spinal cord slice preparation in rats and mice, after dissection from the vertebral column, the dorsal and ventral roots were carefully cut, and the dura mater was carefully removed before blocking the lumbar enlargement. Lumbar enlargements were placed into low melting point agarose gel (3% in oxygenated dissection solution; UltraPure; Invitrogen, Carlsbad, CA, USA) maintained at 37 °C, then placed on ice until agarose solidification. The agarose containing the isolated lumbar enlargement was then secured to a chuck with cyanoacrylate adhesive. 300 μm sagittal spinal cord slices were made using a vibratome (7000 SMZ-2; Campden Instruments Ltd., Leicestershire, UK). Slices were placed in an oxygenated (95% O_2 / 5% CO_2) recovery solution containing (in mM): 92 NMDG, 2.5 KCl, 1.2 NaH_2PO_4, 30 $NaHCO_3$, 20 HEPES, 25 glucose, 5 sodium ascorbate, 2 thiourea, 2 sodium pyruvate, 10 $MgSO_4$, 0.5 $CaCl_2$ (pH = 7.3 – 7.4) at room temperature for 15–20 minutes before being transferred to a solution of oxygenated aCSF containing (in mM): 125 NaCl, 2.5 KCl, 25 $NaHCO_3$, 1 NaH_2PO_4, 25 glucose, 1 $MgCl_2$, 2

$CaCl_2$ at room temperature for 45 – 60 mins. Spinal cord preparations (intact or slice) were then placed into a submersion-type recording chamber (RC-22; Warner Instruments, Hamden, CT, USA), secured onto an upright microscope (BX51WI; Olympus, Center Valley, PA, USA) and maintained under constant perfusion of oxygenated, room temperature aCSF at a rate of 1–3 ml / min unless otherwise indicated.

2.4 Patch-clamp recordings from identified spino-PB neurons

Patch-clamp recording electrodes were constructed using thin-walled, single-filament borosilicate glass (1.5 mm outer diameter, 1.12 mm inner diameter; World Precision Instruments, Inc., Sarasota, FL, USA), using a microelectrode puller (P-97; Sutter Instruments, Novato, CA, USA). Electrode tip resistances ranged from 4 to 6 MΩ, which formed seal resistances > 1 GΩ. For current-clamp recordings of intrinsic excitability, or voltage-clamp recordings of currents evoked by SP (I_{SP}) or the $GABA_BR$ agonist baclofen (I_{Bac}), the internal recording solution was composed of (in mM): 130 K-gluconate, 10 KCl, 10 HEPES, 4 MgATP, 10 Na-phosphocreatine, 0.3 Na-GTP (pH = 7.2–7.4, 295–300 mOsm). For use in voltage-clamp recordings of I_{NALCN}, the internal recording solution was composed of (in mM): 130 Cs-gluconate, 10 CsCl, 1 $CaCl_2$, 11 EGTA, 10 HEPES, 2 MgATP (pH = 7.2–7.4, 300–305 mOsm). Using oblique infrared LED illumination, neurons were visualized in the intact spinal cord preparation as previously described [69,78]. Spino-PB neurons were visualized in the spinal cord slice preparations using infrared-differential interference contrast on the microscope (BX51WI; Olympus, Center Valley, PA, USA).

For recordings of I_{NALCN} and I_{Bac} in DiI-labeled rat spino-PB neurons, approximately one minute after whole-cell configuration was established, series resistance was monitored and maintained at < 20 MΩ. Additionally, all recordings of rat spino-PB I_{NALCN} were obtained under voltage clamp conditions where I_{NALCN} was pharmacologically isolated by bath application of aCSF containing (in μM): 10 NBQX, 20 AP5, 10 gabazine, 0.5 strychnine, 1 TTX and 100 CsCl, applied at 1–3 ml / min to block fast synaptic transmission, voltage-gated Na^+ currents and background K^+ currents, respectively. 1 μM TTX was used in all voltage clamp recordings of I_{NALCN} in order to block Na^+ leak currents mediated by voltage-gated Na^+ channels [12]. In order to avoid I_{Na} fluctuations that have been shown to occur when switching between CO_2-HCO_3^- and HEPES buffering solutions [6], a solution (termed ‘150 bath’) composed of (in mM): 135 NaCl, 14 NaOH, 2.5 KCl, 10 HEPES, 1 NaH_2PO_4, 25 glucose, 1 $MgCl_2$, 2 $CaCl_2$ was used in the recordings of holding current (I_{Hold}). A reduction in external Na^+ concentration ($[Na^+]_e$) was achieved by bath application of a solution (’15 bath’) consisting of (in mM): 111 choline chloride, 14 NaOH, 2.5 KCl, 10 HEPES, 1 NaH_2PO_4, 25 glucose, 1 $MgCl_2$, 2 $CaCl_2$, followed by washout to the ‘150 bath’. I_{Hold} was recorded throughout the entire sequence of perfusion changes. In some experiments, pretreatment of spino-PB neurons with bath-applied 100 μM Gd^{3+} (IC_{50} ~7–10 μM; use at 100 μM ensured ~80–90% inhibition of I_{NALCN} [50]) occurred for ≥ 2 min before $[Na^+]_e$ reduction. To obtain NALCN ramp currents from DiI-labeled rat spino-PB neurons, approximately one minute after attaining the whole-cell configuration, the membrane potential was first hyperpolarized to −100 mV, then depolarizing voltage ramps were applied from −100 mV to −50 mV (at a rate of 0.0125 mV / msec; 5 sweeps). Five trials were

averaged before and after 100 μM Gd^{3+} application and the Gd^{3+}-sensitive component was obtained by electronic subtraction.

For experiments examining I_{SP} and I_{Bac} in rat spinal cord slice preparations containing DiI-labeled spino-PB neurons, 5 μM SP, 100 μM CsCl, 1 μM 1-[2-[(3*S*)-3-(3,4-Dichlorophenyl)-1-[2-[3-(1-methylethoxy)phenyl]acetyl]-3-piperidinyl]ethyl]-4-phenyl-1-azoniabicyclo[2.2.2]octane chloride (SR140333; NK1R antagonist; Tocris Bioscience) or 100 μM R-baclofen (Hello Bio, Princeton, NJ, USA) were applied via bath perfusion. In a subset of voltage-clamp recordings of I_{NALCN}, 50–100 μM $GdCl_3$ or 5 μM SP were applied via bath application. To examine the degree to which SP-evoked NALCN current involved G protein or Src kinase signaling, 1 μM guanosine-5′-O-2-thiodiphosphate (GDPβS; G-protein inhibitor, Tocris Bioscience) or 30 μM 3-(4-chlorophenyl) 1-(1,1-dimethylethyl)-1*H*-pyrazolo[3,4-*d*]pyrimidin-4-amine (PP2; Src kinase inhibitor; Tocris Bioscience) were added to the internal recording solution.

For current-clamp recordings of identified spino-PB neurons in the intact spinal cord preparation from P3–5 rats, spontaneous activity was recorded at the resting membrane potential (RMP) approximately 1 min after whole-cell configuration was established. Cell capacitance was measured using the membrane test function in pClamp 10.4 (Molecular Devices, Sunnyvale, CA, USA). All measurements of intrinsic membrane excitability in both neonatal rats and $NALCN^{f/f}$ mice were taken from RMP. Rheobase was measured by applying depolarizing current steps (5 pA steps, 80 msec duration) until the generation of a single action potential. Duration of action potentials was determined by measuring the elapsed time from the firing threshold to 50% maximum amplitude during the repolarization phase. To examine repetitive firing frequency, sustained depolarizing current steps (10 pA steps, 800 msec duration) were applied via the patch electrode and the instantaneous firing frequency calculated as: mean interspike $interval^{-1}$ at each current step. Measurements of SP-evoked changes in firing frequency of mouse spino-PB neurons were calculated by taking a running average of instantaneous firing frequency before vs. after the bath application of SP. The RMP of neurons exhibiting spontaneous activity after SP administration was calculated by measuring the average membrane potential during the intermittent quiescent periods when the neuron was not firing action potentials.

All membrane voltage measurements were taken after liquid junction potential correction (Clampex; pClamp 10.4, Molecular Devices). Acquired recordings of membrane voltage and currents were filtered at 4 kHz with a −3 dB, 4-pole, lowpass Bessel filter at a digital sampling rate of 20 kHz and stored on a personal computer (Dell Precision T1650, Round Rock, TX, USA) through the use of pClamp 10.4 and a digitizer (Digidata 1440A, Molecular Devices). Offline, currents were digitally filtered using a lowpass Gaussian filter with the −3 dB cutoff set to 1000 Hz (Clampfit software; pClamp 10.4, Molecular Devices).

Brain tissue was collected from each animal used in the electrophysiological experiments and was stored in PFA at 4° C overnight for subsequent histology to verify accurate injection placement in the PBN.

2.5 Imaging

Images of AAV-infected spinal cord sections were obtained by a fluorescent microscope (Olympus BX63, Olympus, Center Valley, PA, USA) using 10x and 20x objective magnification. Single channel z-stack images were then taken with a z-axis separation of 1.0 μm, which were then projected as an extended focus image (EFI) using image acquisition and processing software (CellSens, Olympus Cell Software). All figures were compiled using Photoshop (CS6; Adobe, San Jose, CA, USA).

2.6 Statistical analysis

The statistical analyses in this study are based on the electrophysiological recordings of 210 identified spino-PB neurons from 43 rats of both sexes and 25 mice of both sexes ranging in age from P3–P14. All data were checked for normality using D'Agostino-Pearson omnibus normality tests to ensure that the appropriate statistical tests were used.

Initial characterization of NALCN currents in spinal projection neurons, and their sensitivity to substance P, was conducted in rat in order to complement our prior characterization of leak K^+ currents in lamina I spino-PB neurons [19]. For the experiment outlined in Fig. 1, the effects of $[Na]_e$ reduction on I_{Hold} and RMP were ascertained from the recordings of 17 cells from 5 rats and were analyzed using a Repeated Measures (RM) one-way ANOVA with Holm-Sidak post-tests for multiple comparisons (Prism 7.0 software; GraphPad Software; La Jolla, CA, USA). Additionally, the change in I_{Hold} and RMP in response to $[Na]_e$ reduction after Gd^{3+} occlusion (Control: n = 17 cells, Gd^{3+}: n = 9 cells from 3 rats) was compared using RM one-way ANOVA. To obtain the average Gd^{3+}-sensitive ramp current, 5 cells were recorded from 3 rats, and the resulting linearity of the current was analyzed using a linear regression. The effects Gd^{3+} on spino-PB intrinsic excitability including RMP, spontaneous activity, and rheobase were obtained from the recordings of 8 cells from 4 rats and were compared using paired t-tests.

For the experiment determining SP interaction with NK1R, the data (Control: n = 6 cells from 3 rats; SR140333: n = 3 cells from 1 rat) were analyzed using an unpaired t-test. For the experiment interrogating the influence of GDPβS on I_{Bac}, a total of 9 cells were recorded (n = 3 cells each for control, Cs^+ and GDPβS applications) from 2 rats; the data were analyzed using a one-way ANOVA with Holm-Sidak post-tests, with 'blocker/inhibitor' as the factor. For the experiment which elucidates the signaling pathway involved in SP activation of NALCN channels, the data (Control: n = 9 cells from 7 rats; GDPβS: n = 6 cells from 4 rats; Gd^{3+}: n = 6 cells from 6 rats; PP2: n = 6 cells from 5 rats) were analyzed using a one-way ANOVA with Holm-Sidak post-tests using 'drug/blocker' as a factor. Since the inclusion of 0.3% DMSO into the electrode solution (as a vehicle control for the intracellular administration of PP2) did not significantly alter the magnitude of SP-evoked NALCN currents compared to the standard recording conditions (*data not shown*), these two experimental groups were combined into a single "Control" group for statistical analysis.

The recent generation of $NALCN^{f/f}$ mice [86] provided a valuable opportunity to confirm our major observations via the genetic deletion of NALCN from mouse spinal projection neurons. In the experiment which determined the influence of NALCN channel expression

in spino-PB neurons, the effects of AAV1-GFP (n = 15 cells from 4 mice) vs. AAV1-Cre treatment (n = 14 cells from 6 mice; for rheobase and firing frequency analysis, n = 13 cells) on RMP, spontaneous activity, and rheobase were compared using unpaired t-tests. The firing frequency analysis was performed using a two-way ANOVA with 'virus' and 'stimulation intensity' as factors, followed by Holm-Sidak post-tests for multiple comparisons. In the same experiment, RMP measurements were obtained from the recordings of 9 cells from 3 GFP-infected mice before and after Gd^{3+} application and were compared to the RMP measurements of 8 cells from 4 Cre-infected mice before and after Gd^{3+} using a two-way ANOVA with Holm-Sidak post-tests, using 'blocker' and 'virus' as factors. Similarly, the rheobase measurements of 9 cells from the same 3 GFP-infected mice were compared to the rheobase measurements of 7 cells from the same 4 Cre-infected mice using two-way ANOVA with Holm-Sidak post-tests, using 'blocker' and 'virus' as factors. For the experiment which tested the effect of NALCN channel knockout on SP-evoked firing, the recordings of RMP and spontaneous activity of spino-PB neurons (GFP: n = 8 cells from 6 mice; Cre: n = 8 cells from 5 mice) before and after SP application were compared using two-way ANOVA with Holm-Sidak post-tests, using 'drug' and 'virus' as factors.

The following sections will use 'n' in reference to the number of neurons sampled in each group. Data are expressed as means ± SEM, and p-values < 0.05 resulting from statistical tests were considered statistically significant.

3. Results

3.1 Pharmacological reduction of NALCN current dampens the intrinsic excitability of rat spino-parabrachial (PB) neurons

In order to determine the presence of a Na^+ leak conductance in ascending projection neurons, patch-clamp recordings were obtained from identified rat spino-PB neurons in an intact spinal cord preparation, while the extracellular concentration of Na^+ ($[Na^+]_e$) was reduced to 15 mM ('15 bath'; Fig. 1A). The reduction of $[Na^+]_e$ caused a significant shift in holding current (I_{Hold}) (n = 17, $t_{(16)} = 9.28$, $p < 0.0001$; Fig. 1B, *left*) and a significant hyperpolarization of the RMP (n = 17, $t_{(16)} = 10.75$, $p < 0.0001$; Fig. 1B, *right*). Both the effects on I_{Hold} and RMP were reversible upon washout (WO) (I_{Hold} WO: n = 17, $t_{(16)} = 9.63$, $p < 0.0001$; RMP WO: n = 17, $t_{(16)} = 7.02$, $p < 0.0001$) with a solution containing 150 mM $[Na^+]_e$ ('150 bath'). The sensitivity of the leak Na^+ conductance to a known NALCN blocker, $GdCl_3$, was then examined (Fig. 1C). Bath application of Gd^{3+} significantly reduced the total change in I_{Hold} (Control: n = 17, Gd^{3+}: n = 9, $t_{(24)} = 5.93$, $p < 0.0001$; Fig. 1D) and significantly reduced the magnitude of RMP hyperpolarization (Control: n = 17, Gd^{3+}: n = 9, $t_{(24)} = 7.4$, $p < 0.0001$; Fig. 1E) in response to the reduction in extracellular $[Na^+]_e$.

The properties of the Na^+ leak conductance in identified rat spino-PB neurons were further characterized by voltage-clamp recordings of ramp currents in the absence and presence of Gd^{3+} (Fig. 2A, *left*). The resultant Gd^{3+}-sensitive components of the ramp currents, which were averaged and fitted with a regression line ($y = 0.62x + 9.6$, $r^2 = 0.93$; n = 5; Fig. 2A, *right*), are consistent with I_{NALCN} corresponding to a voltage-independent, non-selective

cation current. Under current-clamp conditions, patch-clamp recordings from spino-PB neurons in the absence and presence of Gd^{3+} were used to determine the effects of NALCN conductance on their intrinsic excitability. A reduction of NALCN conductance in response to Gd^{3+} application significantly hyperpolarized the RMP (Control and Gd^{3+}: n = 8 in each group, $t_{(7)} = 4.7$, p = 0.002; Fig. 2B, 2D), reduced the rate of spontaneous action potential generation (n = 8 in each group, $t_{(7)} = 3.33$, p = 0.013; Fig. 2E), and increased the rheobase (n = 8 in each group, $t_{(7)} = 4.97$, p = 0.0016; Fig. 2C, 2F). Notably, every sampled spino-PB neuron in the above experiments (Figs. 1, 2) exhibited a significant shift in I_{Hold} and intrinsic excitability in response to either '15 bath' or Gd^{3+} application (27 of 27 cells examined), suggesting that NALCN expression is a general feature of immature spino-PB neurons.

3.2 NALCN channel knockout significantly dampens the intrinsic excitability of mouse spino-PB neurons

Although $GdCl_3$ effectively blocks NALCN [50], it has also been shown to inhibit other ion channels [11,32]. Therefore, we employed a genetic strategy to delete NALCN from spino-PB neurons to further support our conclusion that NALCN channels constitutively enhance intrinsic membrane excitability in this population. Following the injections of either AAV1-hSyn-GFP (GFP) or AAV1-hSyn-eGFP·Cre (Cre) into the PBN of $NALCN^{f/f}$ mice (Fig. 3), patch-clamp recordings were subsequently obtained from identified GFP-expressing and Cre-expressing spino-PB neurons in the intact spinal cord preparation (Fig. 4A and 4B). The Cre-dependent knockout of NALCN channels significantly hyperpolarized the RMP (Control: n = 15, Cre: n = 14, $t_{(27)} = 6.48$, p < 0.0001; Fig. 4C), decreased the rate of spontaneous firing (Control: n = 15, Cre: n = 14, $t_{(27)} = 2.92$, p < 0.0001; Fig. 4D), elevated rheobase levels (Control: n = 15, Cre: n = 13, $t_{(26)} = 4.48$, p < 0.0001; Fig. 4E), and had an overall main effect on the repetitive firing frequency (Control: n = 15, Cre: n = 13, $F_{(19,519)} = 25.4$, p < 0.0001; Fig. 4F).

Importantly, NALCN knockout significantly altered the RMP response to Gd^{3+} application (Control: n = 9, Cre: n = 8, $F_{(1,30)} = 13.9$, p = 0.0008; Fig. 4G), as Gd^{3+} significantly hyperpolarized the RMP in control GFP-expressing neurons (Control: n = 9, Gd^{3+}: n = 8, $t_{(30)} = 2.56$, p = 0.03; Fig. 4G, *left*) while having no significant effect on spino-PB neurons after NALCN knockout (Control: n = 9, Gd^{3+}: n = 8, $t_{(30)} = 0.98$, p = 0.98; Fig. 4G, *right*). Similarly, Gd^{3+} application significantly raised rheobase levels in GFP-expressing spino-PB neurons (Control: n = 9, Gd^{3}: n = 7, $t_{(28)} = 2.7$, p = 0.02; Fig. 4H, *left*), but did not affect the rheobase in Cre-expressing projection neurons (Control: n = 9, Gd^{3}: n = 7, $t_{(28)} = 0.11$, p = 0.33; Fig. 4H, *right*). These data strongly support the notion that the previously observed effects of Gd^{3+} on the intrinsic excitability of spino-PB neurons are due to an inhibition of NALCN activity.

3.3 Substance P (SP) activates NALCN in spinal projection neurons via Src kinase signaling

While it has been well-documented that SP can increase the excitability of dorsal horn neurons, the underlying mechanisms are not yet fully understood. As demonstrated previously [17,31,65], SP application evoked a transient inward current in ~93% (14 of 15)

of rat spino-PB neurons in the spinal cord slice preparation, which is consistent with prior studies showing that ~85% of spino-PB neurons exhibit neurokinin-1 receptor (NK1R) immunoreactivity during the neonatal period [56]. As expected, this SP-evoked current was blocked by the selective NK1R antagonist SR140333 (Control: n = 6, SR140333: n = 3, $t_{(7)} = 2.86$, p = 0.024; Fig. 5A–C). Under the above physiological conditions, these inward currents could potentially reflect a decreased conductance through G protein-activated inward-rectifying K^+ (GIRK) channels, an increase in NALCN conductance, or both. To distinguish between these possibilities, we sought to prevent NK1R signaling to GIRK channels by including GDPβS in the intracellular solution (to inhibit G protein activation) and/or bath applying Cs^+ (to block K^+ channels). First, to confirm the inhibition of this signaling pathway, we examined the effects of GDPβS and Cs^+ on the response of spino-PB neurons to the selective $GABA_BR$ agonist R-baclofen (Fig. 5D), which is known to activate GIRK channels in a G protein-dependent manner [34,84]. Baclofen-induced currents (I_{Bac}) were significantly reduced by both extracellular Cs^+ ($t_{(6)} = 5.89$, p = 0.0018; Fig. 5E, G) and intracellular GDPβS ($t_{(6)} = 6.09$, p = 0.0018; Fig. 5F, G) compared to control conditions (n = 3 in each group).

Despite the block of K^+ channels (including GIRK channels) by Cs^+, the bath application of SP still evoked a transient inward current in spino-PB neurons (Fig. 6A) that was significantly reduced by the administration of external Gd^{3+} (Control: n = 9, Gd^{3+}: n = 6, $t_{(23)} = 5.32$, p = 0.0001; Fig. 6B, E), suggesting that the observed current reflected the activation of NALCN channels (and thus termed $I_{SP\text{-}NALCN}$). While the intracellular application of GDPβS blocked I_{Bac} in the prior experiment, it had no significant effect on $I_{SP\text{-}NALCN}$ compared to control measurements (Control: n = 9, GDPβS: n = 6, $t_{(22)} = 1.002$, p = 0.55; Fig. 6C, E) suggesting that G protein signaling was not involved. Meanwhile, as reported previously in hippocampal neurons [51], blocking Src signaling (with intracellular application of PP2) significantly reduced the magnitude of $I_{SP\text{-}NALCN}$ compared to the control group (Control: n = 9, PP2: n = 6, $t_{(23)} = 4.57$, p = 0.0007; Fig. 6D, E).

3.4 SP-evoked excitation of spinal projection neurons critically depends on NALCN expression

The effects of NALCN knockout on SP-evoked firing of mouse spino-PB neurons were evaluated by obtaining current-clamp recordings from both GFP- and Cre-expressing neurons in response to the bath application of SP to spinal cord slices (Fig. 7A–C). Prior to the application of SP, the membrane potential of all sampled neurons was adjusted to approximately −65 mV to account for the hyperpolarizing shift in RMP produced by the genetic deletion of NALCN. Importantly, NALCN knockout significantly ameliorated the depolarizing effects of SP (n = 8 in each group, $F_{(1,28)} = 17.23$, p = 0.0003; Fig. 7D), as SP significantly depolarized the RMP of spino-PB neurons that expressed GFP ($t_{(28)} = 4.16$, p = 0.0006; Fig. 7D, *left*), but had no significant effect on the RMP of spino-PB neurons expressing Cre ($t_{(28)} = 1.7$, p = 0.1; Fig. 7D, *right*). In the control group expressing GFP, SP application could evoke rhythmic burst-firing (Fig. 7A) although the vast majority of spino-PB neurons exhibited an irregular or tonic pattern of discharge (Fig. 7B). Notably, SP evoked a significantly higher rate of action potential generation in projection neurons that

expressed GFP compared to those expressing Cre (n = 8 in each group, $F_{(1,28)} = 4.62$, p = 0.04; Fig. 7E).

4. Discussion

Despite the fundamental importance of spinal projection neurons to the ascending pain pathway [30,80], the ionic mechanisms that modulate their excitability are still incompletely understood. While recent reports demonstrate the influence of the Na^+ leak channel NALCN on the excitability of neurons in the brain [50,51,74], the degree to which these channels shape the output of spinal nociceptive circuits at any stage of life remained unknown. The present results demonstrate, for the first time, that NALCN channels enhance the intrinsic excitability of neonatal spino-parabrachial neurons and their responsiveness to substance P (SP). Collectively, these findings suggest that NALCN channels strongly regulate the flow of nociceptive signals to the developing brain.

Our data clearly indicate that NALCN channels constitutively elevate the intrinsic membrane excitability of spinal projection neurons across multiple species and govern spontaneous firing within these key output cells of the SDH network (Figs. 2, 4, 7). These findings are consistent with prior studies showing that I_{NALCN} increases neuronal excitability and modulates the function of brain circuits involved in respiration, locomotion, chemoreception, and glycolytic sensitivity [22,50,52,53,74]. Our previous work has shown that the level of spontaneous activity (SA) in neonatal projection neurons depends on their supraspinal target, as neurons innervating the periaqueductal gray (PAG) exhibit less spontaneous firing compared to spino-PB neurons [19]. The increased level of SA in spino-PB neurons cannot be attributable to a distinct expression of classic inward-rectifying K^+ (i.e. $K_{ir}2$) leak channels, as the density of $K_{ir}2$ conductance was similar in immature spino-PB vs. spino-PAG projection neurons [19]. Given the considerable heterogeneity of ion channel expression that has been documented among various subpopulations of SDH neurons [18,27,85], it will be interesting to determine whether NALCN channels are differentially expressed across distinct subsets of lamina I projection neurons. Nonetheless, the wide distribution of NALCN mRNA throughout the spinal cord [50] suggests that these channels are found in many subtypes of spinal neurons, although functional studies of NALCN conductance in these other subpopulations remain to be performed. Overall, these results add to the growing body of evidence indicating that voltage-independent channels are powerful determinants of intrinsic excitability within the SDH [14,19,46] and can strongly regulate nociceptive signal transduction and transmission [55,60].

The ability of NALCN channels to shape the activation of projection neurons during early life raises the possibility that alterations in NALCN conductance could have prolonged consequences for the functional organization of spinal and supraspinal pain circuits. Spontaneous firing can influence neurotransmitter expression, axon growth, and synchronization of network activity in the developing spinal cord [4,25,70,83], and also shape the early maturation of brain circuits [28,29,37,49,87]. However, it is important to note that NALCN channels may regulate the firing of projection neurons throughout life. Since the present analysis exclusively focused on the excitability of this population during the early postnatal period, further studies are needed to comprehensively examine how age

may influence NALCN expression and its role in shaping the output of the spinal pain network.

The excitatory effects of the NK1R agonist SP on spinal dorsal horn neurons [13,48,54,64], and other CNS neurons [39,57,89], are required for the sensitization of central nociceptive circuits [31,38,47] which is thought to contribute to pathological pain. SP-evoked depolarization has been shown to rely on G-protein signaling, leading to increased voltage-gated Ca^+ spikes, reduced voltage-gated K^+ currents, and GIRK channel inhibition [42,64,76,79]. The present findings demonstrate that NALCN channels represent an additional downstream target of peptidergic signaling in spino-PB neurons and are in fact essential for SP-mediated excitation of this population. Importantly, our results do not exclude GIRK channels as key effectors of SP signaling in the SDH, as these channels are known to powerfully modulate spinal nociceptive transmission and pain sensitivity [60,61]. It remains highly possible that both the activation of NALCN channels and the closure of GIRK channels are required for the suprathreshold excitation of spinal projection neurons by SP, which warrants further exploration using GIRK knockout mice [60]. SP may thus drive the activation of ascending spinal projection neurons via multiple signaling pathways operating in parallel. The degree to which this may reflect the expression of multiple isoforms of NK1R, which can differ in the relative contribution of β-arrestin and G protein signaling [7,58,82], within projection neurons remains to be determined.

As reported previously in hippocampal and VTA neurons [51], we also found that NALCN currents in spinal projection neurons were increased by SP through a G protein-independent mechanism that involves Src kinase signaling (Figs. 5, 6). Src is known to be upregulated in the dorsal horn under pathological conditions and contributes to pain hypersensitivity under both neuropathic [36] and inflammatory [77] conditions. While Src activity within spinal microglia has been linked to the sensitization of spinal nociceptive circuits [90], it can also potently regulate synaptic function within dorsal horn neurons via the modulation of GluN2B-containing NMDARs [71,75,88]. The activation of Src family kinases in dorsal horn neurons can be triggered by BDNF [15] via mechanisms involving an alteration in intracellular Cl^- homeostasis [26]. Interestingly, Src signaling also facilitates the potentiation of NMDARs by intracellular sodium [88]. Therefore, Src activation occurring downstream of NK1R activation [51] could potentially enhance NMDAR function in spinal projection neurons both directly, by altering the phosphorylation of the GluN2B subunit [26], and indirectly via an increased Na^+ influx through NALCN channels. This would be predicted to exert a significant influence on activity-dependent synaptic plasticity in the SDH, given the critical contribution of NMDARs to multiple forms of long-term potentiation (LTP) in lamina I projection neurons [31,45].

The ablation of NK1R-expressing spinal neurons, which include projection neurons, attenuates mechanical and thermal hyperalgesia in response to capsaicin, inflammation or nerve injury [40,56,59,68]. However, the functional consequences of NALCN deletion within spino-parabrachial neurons for behavioral pain sensitivity remain to be determined. An obvious obstacle to addressing this key issue using the present experimental approach is that, while the NALCN knockout is selective for ascending projection neurons at the level of the spinal cord, significant deletion of NALCN also occurs in the parabrachial nucleus near

the site of AAV-Cre administration. Obtaining a selective knockout of NALCN from spinal projection neurons will necessitate the development of new experimental tools to allow for the application of an intersectional genetic strategy, as recently employed in the study of interneurons within the spinal dorsal horn [5,16]. Alternatively, the injection of an AAV vector encoding a tamoxifen-inducible Cre recombinase could be combined with local injections of the tamoxifen metabolite (z)-4-hydroxytamoxifen into the lumbar SDH in order to drive a localized activation of Cre, as described elsewhere in the CNS [1,41]. If the selective knockout of NALCN from spinal projection neurons can be achieved, it would be of great interest to examine the subsequent effects on both reflexive and non-reflexive assays of pain sensitivity, as the latter measures may yield more insight into the ongoing pain seen in human patients [62,63]. Certainly, the known importance of the spino-parabrachio-amygdaloid pathway for the regulation of the emotional-affective dimensions of pain [2,23,24,67] might predict a significant effect of NALCN knockout in projection neurons on pain aversion or pain-associated depressive behaviors [3,35].

In conclusion, the current results demonstrate that the Na^+ leak channel NALCN is a strong regulator of intrinsic membrane excitability in developing spino-parabrachial neurons and plays a critical role in their activation by the neuropeptide Substance P. These findings therefore suggest that any changes in NALCN conductance within this neuronal population, such as those evoked by Src kinase signaling, will have profound consequences for the level of ascending nociceptive transmission to supraspinal pain networks.

Acknowledgments

The authors report no conflicts of interest in the preparation and submission of this manuscript. This work was supported by the National Institutes of Health (NS072202 to MLB). The authors would like to thank E. Serafin and Dr. Wenrui Xie for technical support, and Drs. Matthieu Flourakis and Ravi Allada for assistance in obtaining the $NALCN^{f/f}$ mice.

References

1. Benedykcinska A, Ferreira A, Lau J, Broni J, Richard-Loendt A, Henriquez NV, Brandner S. Generation of brain tumours in mice by Cre-mediated recombination of neural progenitors in situ with the tamoxifen metabolite endoxifen. Disease models & mechanisms. 2016; 9(2):211–220. [PubMed: 26704996]
2. Bernard JF, Besson JM. The spino(trigemino)pontoamygdaloid pathway: electrophysiological evidence for an involvement in pain processes. J Neurophysiol. 1990; 63(3):473–490. [PubMed: 2329357]
3. Blackburn-Munro G, Blackburn-Munro RE. Chronic Pain, Chronic Stress and Depression: Coincidence or Consequence? Journal of Neuroendocrinology. 2001; 13(12):1009–1023. [PubMed: 11722697]
4. Borodinsky LN, Root CM, Cronin JA, Sann SB, Gu X, Spitzer NC. Activity-dependent homeostatic specification of transmitter expression in embryonic neurons. Nature. 2004; 429(6991):523–530. [PubMed: 15175743]
5. Bourane S, Duan B, Koch SC, Dalet A, Britz O, Garcia-Campmany L, Kim E, Cheng L, Ghosh A, Ma Q, Goulding M. Gate control of mechanical itch by a subpopulation of spinal cord interneurons. Science. 2015; 350(6260):550–554. [PubMed: 26516282]
6. Bruehl C, Witte OW. Relation between bicarbonate concentration and voltage dependence of sodium currents in freshly isolated CA1 neurons of the rat. J Neurophysiol. 2003; 89(5):2489–2498. [PubMed: 12611966]

7. Cahill TJ 3rd, Thomsen AR, Tarrasch JT, Plouffe B, Nguyen AH, Yang F, Huang LY, Kahsai AW, Bassoni DL, Gavino BJ, Lamerdin JE, Triest S, Shukla AK, Berger B, Little Jt, Antar A, Blanc A, Qu CX, Chen X, Kawakami K, Inoue A, Aoki J, Steyaert J, Sun JP, Bouvier M, Skiniotis G, Lefkowitz RJ. Distinct conformations of GPCR-beta-arrestin complexes mediate desensitization, signaling, and endocytosis. Proc Natl Acad Sci U S A. 2017; 114(10):2562–2567. [PubMed: 28223524]
8. Cao YQ, Mantyh PW, Carlson EJ, Gillespie AM, Epstein CJ, Basbaum AI. Primary afferent tachykinins are required to experience moderate to intense pain. Nature. 1998; 392(6674):390–394. [PubMed: 9537322]
9. Caterina MJ, Leffler A, Malmberg AB, Martin WJ, Trafton J, Petersen-Zeitz KR, Koltzenburg M, Basbaum AI, Julius D. Impaired nociception and pain sensation in mice lacking the capsaicin receptor. Science. 2000; 288(5464):306–313. [PubMed: 10764638]
10. Chen Q, Roeder Z, Li MH, Zhang Y, Ingram SL, Heinricher MM. Optogenetic Evidence for a Direct Circuit Linking Nociceptive Transmission through the Parabrachial Complex with Pain-Modulating Neurons of the Rostral Ventromedial Medulla (RVM). eNeuro. 2017; 4(3)
11. Clapham DE. SnapShot: mammalian TRP channels. Cell. 2007; 129:220. [PubMed: 17418797]
12. Dai Y, Jordan LM. Tetrodotoxin-, dihydropyridine-, and riluzole-resistant persistent inward current: novel sodium channels in rodent spinal neurons. J Neurophysiol. 2011; 106(3):1322–1340. [PubMed: 21653721]
13. De Koninck Y, Henry JL. Substance P-mediated slow excitatory postsynaptic potential elicited in dorsal horn neurons in vivo by noxious stimulation. Proc Natl Acad Sci U S A. 1991; 88(24): 11344–11348. [PubMed: 1722327]
14. Derjean D, Bertrand S, Le Masson G, Landry M, Morisset V, Nagy F. Dynamic balance of metabotropic inputs causes dorsal horn neurons to switch functional states. Nature neuroscience. 2003; 6(3):274–281. [PubMed: 12592405]
15. Ding X, Cai J, Li S, Liu XD, Wan Y, Xing GG. BDNF contributes to the development of neuropathic pain by induction of spinal long-term potentiation via SHP2 associated GluN2B-containing NMDA receptors activation in rats with spinal nerve ligation. Neurobiol Dis. 2015; 73:428–451. [PubMed: 25447233]
16. Duan B, Cheng L, Bourane S, Britz O, Padilla C, Garcia-Campmany L, Krashes M, Knowlton W, Velasquez T, Ren X, Ross S, Lowell BB, Wang Y, Goulding M, Ma Q. Identification of spinal circuits transmitting and gating mechanical pain. Cell. 2014; 159(6):1417–1432. [PubMed: 25467445]
17. Emonds-Alt X, Doutremepuich J, Heaulme M, Neliat G, Santucci V, Steinberg R, Vilain P, Bichon D, Ducoux J, Proeitto V, Van Broec D, Soubrie P, Le Fur G, Beliere J. In vitro and in vivo biological activities of SR140333, a novel potent non-peptide tachykinin NK 1 receptor antagonist. Eur J Pharmacol. 1993; 250:403–413. [PubMed: 7509286]
18. Engelman HS, Allen TB, MacDermott AB. The distribution of neurons expressing calcium-permeable AMPA receptors in the superficial laminae of the spinal cord dorsal horn. The Journal of neuroscience : the official journal of the Society for Neuroscience. 1999; 19(6):2081–2089. [PubMed: 10066261]
19. Ford NC, Baccei ML. Inward-rectifying K+ (Kir2) leak conductance dampens the excitability of lamina I projection neurons in the neonatal rat. Neuroscience. 2016; 339:502–510. [PubMed: 27751963]
20. Francois A, Low SA, Sypek EI, Christensen AJ, Sotoudeh C, Beier KT, Ramakrishnan C, Ritola KD, Sharif-Naeini R, Deisseroth K, Delp SL, Malenka RC, Luo L, Hantman AW, Scherrer G. A Brainstem-Spinal Cord Inhibitory Circuit for Mechanical Pain Modulation by GABA and Enkephalins. Neuron. 2017; 93(4):822–839. e826. [PubMed: 28162807]
21. Gamse R. Capsaicin and nociception in the rat and mouse. Possible role of substance P. Naunyn Schmiedebergs Arch Pharmacol. 1982; 320(3):205–216. [PubMed: 6182473]
22. Gao S, Xie L, Kawano T, Po MD, Guan S, Zhen M, Pirri JK, Alkema MJ. The NCA sodium leak channel is required for persistent motor circuit activity that sustains locomotion. Nat Commun. 2015; 6:6323. [PubMed: 25716181]

23. Han JS, Neugebauer V. mGluR1 and mGluR5 antagonists in the amygdala inhibit different components of audible and ultrasonic vocalizations in a model of arthritic pain. Pain. 2005; 113(1–2):211–222. [PubMed: 15621382]
24. Han S, Soleiman MT, Soden ME, Zweifel LS, Palmiter RD. Elucidating an Affective Pain Circuit that Creates a Threat Memory. Cell. 2015; 162(2):363–374. [PubMed: 26186190]
25. Hanson MG, Landmesser LT. Normal patterns of spontaneous activity are required for correct motor axon guidance and the expression of specific guidance molecules. Neuron. 2004; 43(5): 687–701. [PubMed: 15339650]
26. Hildebrand ME, Xu J, Dedek A, Li Y, Sengar AS, Beggs S, Lombroso PJ, Salter MW. Potentiation of Synaptic GluN2B NMDAR Currents by Fyn Kinase Is Gated through BDNF-Mediated Disinhibition in Spinal Pain Processing. Cell reports. 2016; 17(10):2753–2765. [PubMed: 27926876]
27. Hu HJ, Gereau RWt. Metabotropic glutamate receptor 5 regulates excitability and Kv4. 2-containing K(+) channels primarily in excitatory neurons of the spinal dorsal horn. J Neurophysiol. 2011; 105(6):3010–3021. [PubMed: 21451053]
28. Hua JY, Smear MC, Baier H, Smith SJ. Regulation of axon growth in vivo by activity-based competition. Nature. 2005; 434(7036):1022–1026. [PubMed: 15846347]
29. Hubel DH, Wiesel TN. The period of susceptibility to the physiological effects of unilateral eye closure in kittens. J Physiol. 1970; 206(2):419–436. [PubMed: 5498493]
30. Hylden JL, Anton F, Nahin RL. Spinal lamina I projection neurons in the rat: collateral innervation of parabrachial area and thalamus. Neuroscience. 1989; 28(1):27–37. [PubMed: 2548118]
31. Ikeda H, Stark J, Fischer H, Wagner M, Drdla R, Jager T, Sandkühler J. Synaptic amplifier of inflammatory pain in the spinal dorsal horn. Science. 2006; 312(5780):1659–1662. [PubMed: 16778058]
32. Ishibashi H, Hirao K, Yamaguchi J, Nabekura J. Inhibition of chloride outward transport by gadolinium in cultured rat spinal cord neurons. Neurotoxicology. 2009; 30(1):155–159. [PubMed: 19007810]
33. Jhamandas JH, Petrov T, Harris KH, Vu T, Krukoff TL. Parabrachial nucleus projection to the amygdala in the rat: electrophysiological and anatomical observations. Brain Res Bull. 1996; 39(2):115–126. [PubMed: 8846113]
34. Kangrga I, Jiang MC, Randic M. Actions of (−)-baclofen on rat dorsal horn neurons. Brain research. 1991; 562(2):265–275. [PubMed: 1685343]
35. Kask K, Berthold M, Bartfai T. Galanin receptors: Involvement in feeding, pain, depression and Alzheimer's disease. Life Sciences. 1997; 60(18):1523–1533. [PubMed: 9126874]
36. Katsura H, Obata K, Mizushima T, Sakurai J, Kobayashi K, Yamanaka H, Dai Y, Fukuoka T, Sakagami M, Noguchi K. Activation of Src-family kinases in spinal microglia contributes to mechanical hypersensitivity after nerve injury. The Journal of neuroscience : the official journal of the Society for Neuroscience. 2006; 26(34):8680–8690. [PubMed: 16928856]
37. Katz LC, Shatz CJ. Synaptic activity and the construction of cortical circuits. Science. 1996; 274(5290):1133–1138. [PubMed: 8895456]
38. Khasabov S, Ghilardi JR, Peters CM, Mantyh PW, Simone DA. Spinal neurons that possess the substance P receptor are required for the development of central sensitization. The Journal of neuroscience : the official journal of the Society for Neuroscience. 2002; 22(20):9086–9098. [PubMed: 12388616]
39. Kim BJ, Chang IY, Choi S, Jun JY, Jeon JH, Xu WX, Kwon YK, Ren D, So I. Involvement of Na(+)-leak channel in substance P-induced depolarization of pacemaking activity in interstitial cells of Cajal. Cell Physiol Biochem. 2012; 29(3–4):501–510. [PubMed: 22508057]
40. King T, Qu C, Okun A, Mercado R, Ren J, Brion T, Lai J, Porreca F. Contribution of afferent pathways to nerve injury-induced spontaneous pain and evoked hypersensitivity. Pain. 2011; 152(9):1997–2005. [PubMed: 21620567]
41. Kohro Y, Sakaguchi E, Tashima R, Tozaki-Saitoh H, Okano H, Inoue K, Tsuda M. A new minimally-invasive method for microinjection into the mouse spinal dorsal horn. Scientific reports. 2015; 5:14306. [PubMed: 26387932]

42. Koike-Tani M, Collins JM, Kawano T, Zhao P, Zhao Q, Kozasa T, Nakajima S, Nakajima Y. Signal transduction pathway for the substance P-induced inhibition of rat Kir3 (GIRK) channel. J Physiol. 2005; 564(Pt 2):489–500. [PubMed: 15731196]
43. Lee JH, Cribbs LL, Perez-Reyes E. Cloning of a novel four repeat protein related to voltage-gated sodium and calcium channels. FEBS Lett. 1999; 445(2–3):231–236. [PubMed: 10094463]
44. Li J, Baccei ML. Neonatal Tissue Damage Promotes Spike Timing-Dependent Synaptic Long-Term Potentiation in Adult Spinal Projection Neurons. The Journal of neuroscience : the official journal of the Society for Neuroscience. 2016; 36(19):5405–5416. [PubMed: 27170136]
45. Li J, Baccei ML. Functional Organization of Cutaneous and Muscle Afferent Synapses onto Immature Spinal Lamina I Projection Neurons. The Journal of neuroscience : the official journal of the Society for Neuroscience. 2017; 37(6):1505–1517. [PubMed: 28069928]
46. Li J, Blankenship ML, Baccei ML. Inward-rectifying potassium (Kir) channels regulate pacemaker activity in spinal nociceptive circuits during early life. The Journal of neuroscience : the official journal of the Society for Neuroscience. 2013; 33(8):3352–3362. [PubMed: 23426663]
47. Liu X, Sandkühler J. Characterization of long-term potentiation of C-fiber-evoked potentials in spinal dorsal horn of adult rat: essential role of NK1 and NK2 receptors. J Neurophysiol. 1997; 78(4):1973–1982. [PubMed: 9325365]
48. Liu XG, Sandkühler J. The effects of extrasynaptic substance P on nociceptive neurons in laminae I and II in rat lumbar spinal dorsal horn. Neuroscience. 1995; 68(4):1207–1218. [PubMed: 8544994]
49. Lorenzetto E, Caselli L, Feng G, Yuan W, Nerbonne JM, Sanes JR, Buffelli M. Genetic perturbation of postsynaptic activity regulates synapse elimination in developing cerebellum. Proc Natl Acad Sci U S A. 2009; 106(38):16475–16480. [PubMed: 19805323]
50. Lu B, Su Y, Das S, Liu J, Xia J, Ren D. The neuronal channel NALCN contributes resting sodium permeability and is required for normal respiratory rhythm. Cell. 2007; 129(2):371–383. [PubMed: 17448995]
51. Lu B, Su Y, Das S, Wang H, Wang Y, Liu J, Ren D. Peptide neurotransmitters activate a cation channel complex of NALCN and UNC-80. Nature. 2009; 457(7230):741–744. [PubMed: 19092807]
52. Lu TZ, Feng ZP. A sodium leak current regulates pacemaker activity of adult central pattern generator neurons in Lymnaea stagnalis. PLoS One. 2011; 6(4):e18745. [PubMed: 21526173]
53. Lutas A, Lahmann C, Soumillon M, Yellen G. The leak channel NALCN controls tonic firing and glycolytic sensitivity of substantia nigra pars reticulata neurons. eLife. 2016; 5(e15271)
54. Luz LL, Szucs P, Safronov BV. Peripherally driven low-threshold inhibitory inputs to lamina I local-circuit and projection neurones: a new circuit for gating pain responses. J Physiol. 2014; 592(7):1519–1534. [PubMed: 24421354]
55. Ma C, Rosenzweig J, Zhang P, Johns DC, LaMotte RH. Expression of inwardly rectifying potassium channels by an inducible adenoviral vector reduced the neuronal hyperexcitability and hyperalgesia produced by chronic compression of the spinal ganglion. Mol Pain. 2010; 6(1):65. [PubMed: 20923570]
56. Man SH, Geranton SM, Hunt SP. Lamina I NK1 expressing projection neurones are functional in early postnatal rats and contribute to the setting up of adult mechanical sensory thresholds. Mol Pain. 2012; 8(1):35. [PubMed: 22540287]
57. Mantyh PW, Allen CJ, Ghilardi JR, Rogers SD, Mantyh CR, Liu H, Basbaum AI, Vigna SR, Maggio JE. Rapid endocytosis of a G protein-coupled receptor: substance P evoked internalization of its receptor in the rat striatum in vivo. Proc Natl Acad Sci U S A. 1995; 92(7):2622–2626. [PubMed: 7535928]
58. Mantyh PW, Rogers SD, Ghilardi JR, Maggio JE, Mantyh CR, Vigna SR. Differential expression of two isoforms of the neurokinin-1 (substance P) receptor in vivo. Brain research. 1996; 719(1–2):8–13. [PubMed: 8782857]
59. Mantyh PW, Rogers SD, Honore P, Allen BJ, Ghilardi JR, Li J, Daughters RS, Lappi DA, Wiley RG, Simone DA. Inhibition of hyperalgesia by ablation of lamina I spinal neurons expressing the substance P receptor. Science. 1997; 278(5336):275–279. [PubMed: 9323204]

60. Marker CL, Cintora SC, Roman MI, Stoffel M, Wickman K. Hyperalgesia and blunted morphine analgesia in G protein-gated potassium channel subunit knockout mice. Neuroreport. 2002; 13(18): 2509–2513. [PubMed: 12499858]
61. Marker CL, Stoffel M, Wickman K. Spinal G-protein-gated K+ channels formed by GIRK1 and GIRK2 subunits modulate thermal nociception and contribute to morphine analgesia. The Journal of neuroscience : the official journal of the Society for Neuroscience. 2004; 24(11):2806–2812. [PubMed: 15028774]
62. Mogil JS. Animal models of pain: progress and challenges. Nature reviews Neuroscience. 2009; 10(4):283–294. [PubMed: 19259101]
63. Mogil JS, Crager SE. What should we be measuring in behavioral studies of chronic pain in animals? Pain. 2004; 112(1–2):12–15. [PubMed: 15494180]
64. Murase K, Randic M. Actions of substance P on rat spinal dorsal horn neurones. J Physiol. 1984; 346:203–217. [PubMed: 6199493]
65. Murase K, Ryu PD, Randic M. Excitatory and inhibitory amino acids and peptide-induced responses in acutely isolated rat spinal dorsal horn neurons. Neurosci Lett. 1989; 103(1):56–63. [PubMed: 2476693]
66. Nagy JI, Iversen LL, Goedert M, Chapman D, Hunt SP. Dose-dependent effects of capsaicin on primary sensory neurons in the neonatal rat. The Journal of neuroscience : the official journal of the Society for Neuroscience. 1983; 3(2):399–406. [PubMed: 6185658]
67. Neugebauer V, Li W, Bird GC, Han JS. The amygdala and persistent pain. Neuroscientist. 2004; 10(3):221–234. [PubMed: 15155061]
68. Nichols ML, Allen BJ, Rogers SD, Ghilardi JR, Honore P, Luger NM, Finke MP, Li J, Lappi DA, Simone DA, Mantyh PW. Transmission of chronic nociception by spinal neurons expressing the substance P receptor. Science. 1999; 286(5444):1558–1561. [PubMed: 10567262]
69. Safronov BV, Pinto V, Derkach VA. High-resolution single-cell imaging for functional studies in the whole brain and spinal cord and thick tissue blocks using light-emitting diode illumination. J Neurosci Methods. 2007; 164:292–298. [PubMed: 17586052]
70. Saint-Amant L, Drapeau P. Synchronization of an embryonic network of identified spinal interneurons solely by electrical coupling. Neuron. 2001; 31(6):1035–1046. [PubMed: 11580902]
71. Salter MW, Pitcher GM. Dysregulated Src upregulation of NMDA receptor activity: a common link in chronic pain and schizophrenia. FEBS J. 2012; 279(1):2–11. [PubMed: 21985289]
72. Santos ARS, Calixto JB. Further evidence for the involvement of tachykinin receptor subtypes in formalin and capsaicin models of pain in mice. Neuropeptides. 1997; 31(4):381–389. [PubMed: 9308027]
73. Sato M, Ito M, Nagase M, Sugimura YK, Takahashi Y, Watabe AM, Kato F. The lateral parabrachial nucleus is actively involved in the acquisition of fear memory in mice. Molecular brain. 2015; 8(22):22. [PubMed: 25888401]
74. Shi Y, Abe C, Holloway BB, Shu S, Kumar NN, Weaver JL, Sen J, Perez-Reyes E, Stornetta RL, Guyenet PG, Bayliss DA. Nalcn Is a “Leak” Sodium Channel That Regulates Excitability of Brainstem Chemosensory Neurons and Breathing. The Journal of neuroscience : the official journal of the Society for Neuroscience. 2016; 36(31):8174–8187. [PubMed: 27488637]
75. Slack S, Battaglia A, Cibert-Goton V, Gavazzi I. EphrinB2 induces tyrosine phosphorylation of NR2B via Src-family kinases during inflammatory hyperalgesia. Neuroscience. 2008; 156(1):175–183. [PubMed: 18694808]
76. Stanfield PR, Nakajima Y, Yamaguchi K. Substance P raises neuronal membrane excitability by reducing inward rectification. Nature. 1985; 315(6019):498–501. [PubMed: 2582270]
77. Suo ZW, Yang X, Li L, Liu YN, Shi L, Hu XD. Inhibition of protein tyrosine phosphatases in spinal dorsal horn attenuated inflammatory pain by repressing Src signaling. Neuropharmacology. 2013; 70:122–130. [PubMed: 23376245]
78. Szűcs P, Pinto V, Safronov BV. Advanced technique of infrared LED imaging of unstained cells and intracellular structures in isolated spinal cord, brainstem, ganglia and cerebellum. J Neurosci Methods. 2009; 177:369–380. [PubMed: 19014968]

79. Thorn Perez C, Hill RH, Grillner S. Substance P Depolarizes Lamprey Spinal Cord Neurons by Inhibiting Background Potassium Channels. PLoS One. 2015; 10(7):e0133136. [PubMed: 26197458]
80. Todd AJ. Neuronal circuitry for pain processing in the dorsal horn. Nature reviews Neuroscience. 2010; 11(12):823–836. [PubMed: 21068766]
81. Todd AJ, McGill MM, Shehab SAS. Neurokinin 1 receptor expression by neurons in laminae I, III and IV of the rat spinal dorsal horn that project to the brainstem. The European journal of neuroscience. 2000; 12(2):689–700. [PubMed: 10712649]
82. Valentin-Hansen L, Frimurer TM, Mokrosinski J, Holliday ND, Schwartz TW. Biased Gs versus Gq proteins and beta-arrestin signaling in the NK1 receptor determined by interactions in the water hydrogen bond network. The Journal of biological chemistry. 2015; 290(40):24495–24508. [PubMed: 26269596]
83. Wilhelm JC, Rich MM, Wenner P. Compensatory changes in cellular excitability, not synaptic scaling, contribute to homeostatic recovery of embryonic network activity. Proc Natl Acad Sci U S A. 2009; 106(16):6760–6765. [PubMed: 19346492]
84. Wydeven N, Marron Fernandez de Velasco E, Du Y, Benneyworth MA, Hearing MC, Fischer RA, Thomas MJ, Weaver CD, Wickman K. Mechanisms underlying the activation of G-protein-gated inwardly rectifying K+ (GIRK) channels by the novel anxiolytic drug, ML297. Proc Natl Acad Sci U S A. 2014; 111(29):10755–10760. [PubMed: 25002517]
85. Yasaka T, Tiong SY, Hughes DI, Riddell JS, Todd AJ. Populations of inhibitory and excitatory interneurons in lamina II of the adult rat spinal dorsal horn revealed by a combined electrophysiological and anatomical approach. Pain. 2010; 151(2):475–488. [PubMed: 20817353]
86. Yeh SY, Huang WH, Wang W, Ward CS, Chao ES, Wu Z, Tang B, Tang J, Sun JJ, Esther van der Heijden M, Gray PA, Xue M, Ray RS, Ren D, Zoghbi HY. Respiratory Network Stability and Modulatory Response to Substance P Require Nalcn. Neuron. 2017; 94(2):294–303. e294. [PubMed: 28392070]
87. Yu C, Power J, Barnea G, O'Donnell S, Brown H, Osborne J, Axel R, Gogos J. Spontaneous neural activity is required for the establishment and maintenance of the olfactory sensory map. Neuron. 2004; 42(4):553–566. [PubMed: 15157418]
88. Yu XM, Salter MW. Src, a molecular switch governing gain control of synaptic transmission mediated by N-methyl-D-aspartate receptors. Proceedings of the National Academy of Sciences. 1999; 96(14):7697–7704.
89. Zhang L, Hammond DL. Substance P enhances excitatory synaptic transmission on spinally projecting neurons in the rostral ventromedial medulla after inflammatory injury. J Neurophysiol. 2009; 102(2):1139–1151. [PubMed: 19494188]
90. Zhong Y, Zhou LJ, Ren WJ, Xin WJ, Li YY, Zhang T, Liu XG. The direction of synaptic plasticity mediated by C-fibers in spinal dorsal horn is decided by Src-family kinases in microglia: the role of tumor necrosis factor-alpha. Brain Behav Immun. 2010; 24(6):874–880. [PubMed: 20116424]

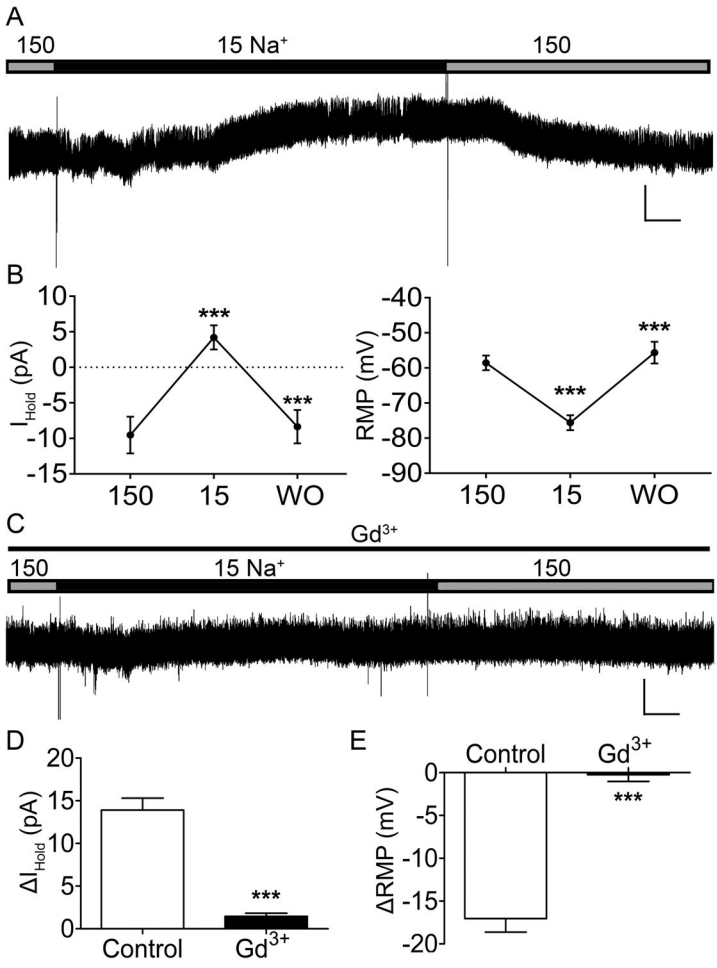

Figure 1. Neonatal rat spinal projection neurons express a NALCN-like Na^+ leak current that is sensitive to Gd^{3+}

A. Representative trace of holding current (I_{Hold}) in response to a reduction of extracellular Na^+ concentration ($[Na^+]_e$) to 15 mM. Gray bar, 150 mM $[Na^+]_e$; Black bar, 15 mM $[Na^+]_e$. Scale bars: 20 pA, 20 s. **B.** A reduction of $[Na^+]_e$ to 15 mM caused a significant positive shift in I_{Hold} (13.73 ± 1.48 pA; n = 17, $t_{(16)}$ = 9.28, *** p < 0.0001, RM one-way ANOVA; left panel), and significantly hyperpolarized the resting membrane potential (RMP; 17.04 ± 1.59 mV; n = 17, $t_{(16)}$ = 10.75, *** p < 0.0001, RM one-way ANOVA; right panel). Both effects were reversible upon washout (WO) with the normal bath solution (*** p < 0.0001, RM one-way ANOVA with Holm-Sidak post-test). **C.** Representative trace of I_{Hold} in response to a reduction of $[Na^+]_e$ after Gd^{3+} occlusion. Thin black line, 100 μM Gd^{3+} application. Scale bars: 20 pA, 20 s. **D.** Gd^{3+} application significantly reduced the overall change in I_{Hold} in response to $[Na^+]_e$ reduction (by 12.27 ± 2.07 pA; Control: n = 17, Gd^{3+}: n = 9; $t_{(24)}$ = 5.93, *** p < 0.0001, unpaired t-test). **E.** RMP hyperpolarization in response to 15 mM $[Na^+]_e$ was prevented by the application of Gd^{3+} (Control: n = 17, Gd^{3+}: n = 9; $t_{(24)}$ = 7.4, *** p < 0.0001, unpaired t-test).

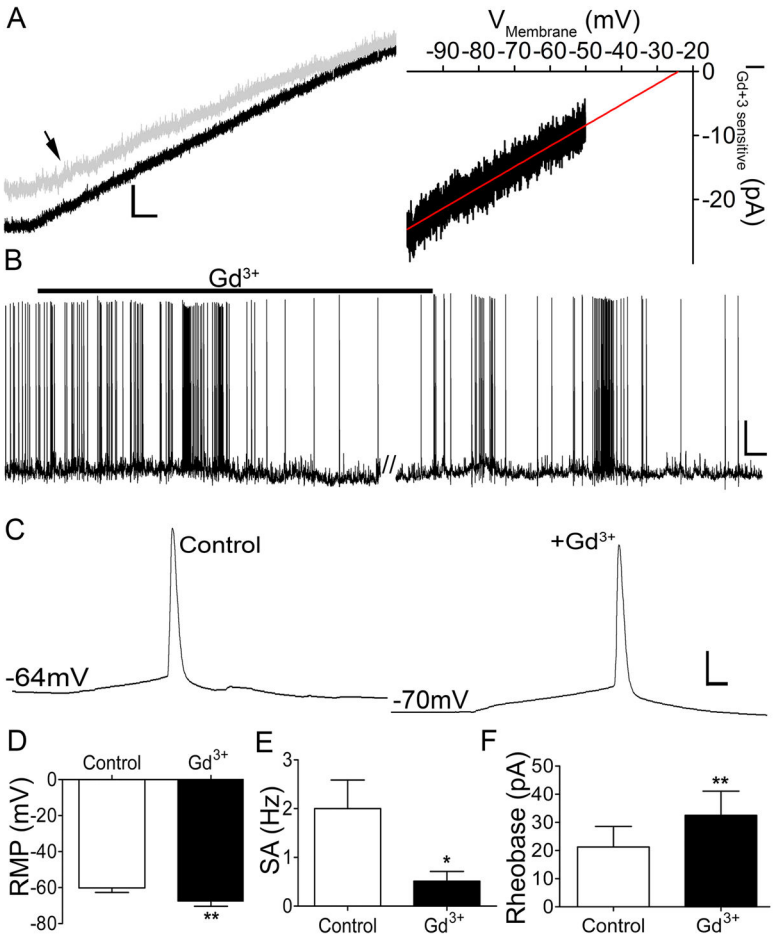

Figure 2. Pharmacological reduction of I_{NALCN} dampens the intrinsic excitability of immature spino-PB neurons

A. Left panel: representative trace of whole-cell ramp current before (black trace) and after 100 μM Gd^{3+}application (gray trace indicated by black arrow). Scale bars: 20 pA, 125 msec. Right panel: average of Gd^{3+}-sensitive ramp current fitted with a regression line (y = 0.62x + 9.6, r^2 = 0.93; n = 5), consistent with a voltage-independent, mixed cation conductance. **B.** Representative trace of spontaneous activity in a rat spino-PB neuron illustrating a reduction in firing after the bath application of 10 μM Gd^{3+}. Scale bars: 20 mV, 20 s. **C.** Representative examples of action potential discharge at rheobase before (left panel) and after (right panel) Gd^{3+} application. Scale bars: 20 mV, 10 msec. **D – F.** 10 μM Gd^{3+} application significantly hyperpolarized RMP (by 7.29 ± 1.55 mV; n = 8, $t_{(7)}$ = 4.7, ** p = 0.002, paired t-test; **D**), reduced the frequency of spontaneous action potential generation (by 1.49 ± 0.44 Hz; n = 8, $t_{(7)}$ = 3.33, * p = 0.013, paired t-test; **E**), and increased rheobase levels (by 11.25 ± 2.27 pA; n = 8, $t_{(7)}$ = 4.97, ** p = 0.0016, paired t-test; **F**) in spino-PB neurons.

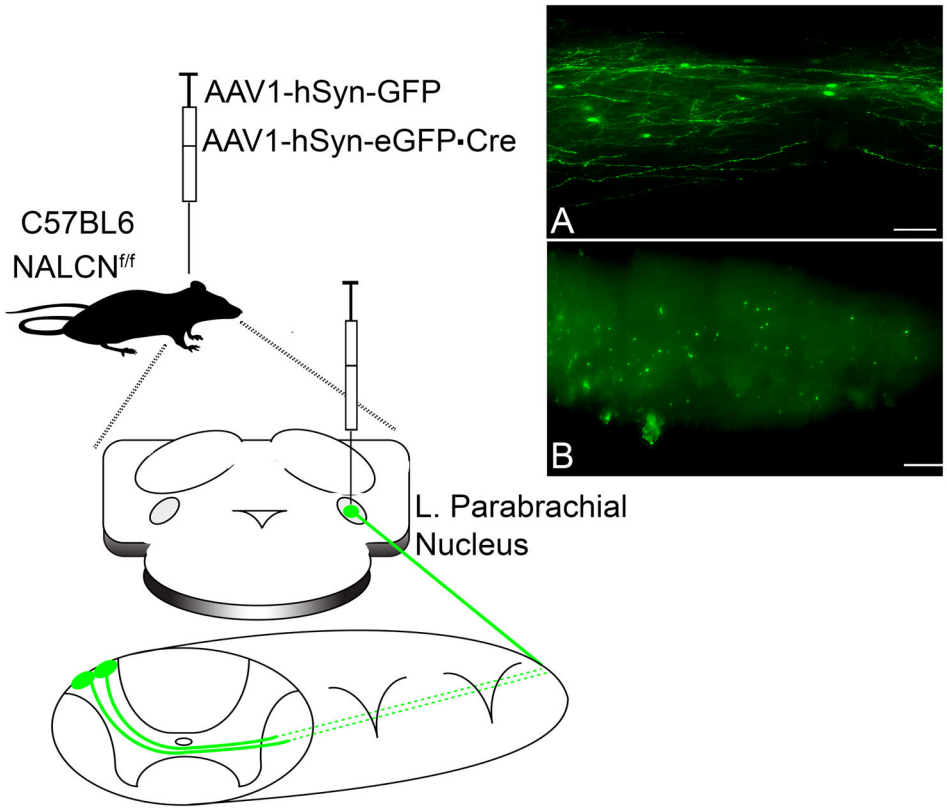

Figure 3. Genetic strategy to delete NALCN from ascending spinal projection neurons

P3 C57BL6 mice containing loxP sites flanking the NALCN gene (NALCN$^{f/f}$) were injected with control AAV1-hSyn-GFP or AAV1-hSyn-eGFP·Cre into the lateral parabrachial nucleus (PBN). **A**. Representative image of a 25 μm horizontal section of lamina I from a P17 mouse spinal cord after 200 nl intracranial injection of AAV1-hSyn-GFP into the parabrachial nucleus (PB) on P3, illustrating the cystolic expression of GFP within lamina I spino-PB neurons. Scale bar: 50 μm. **B**. Representative image of a 50 μm horizontal section of lamina I from a P17 mouse spinal cord after 200 nl intracranial injection of AAV1-hSyn-eGFP·Cre into the PB at P3, which results in expression of the Cre-GFP fusion protein in the nucleus of lamina I spino-PB neurons. Scale bar, 200 μm.

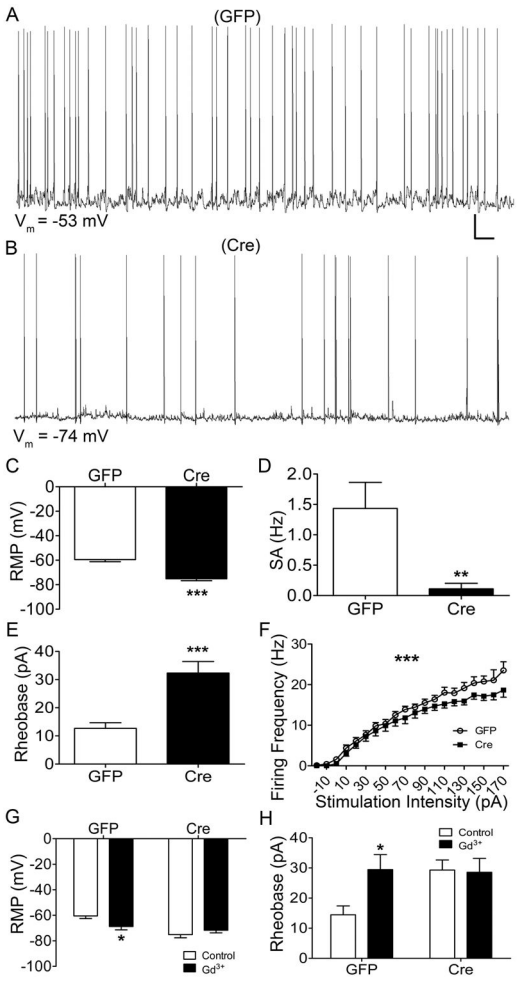

Figure 4. NALCN knockout decreases the intrinsic excitability of spino-PB neurons

A – B. Representative traces of spontaneous activity from control GFP (**A**; n = 15) and NALCN knockout (**B**) spino-PB neurons (n = 14 for comparisons in **C** and **D**; and n = 13 for comparisons in **E** and **F**). Scale bars: 10 mV, 10 s. **C – F:** NALCN knockout in mouse projection neurons resulted in significant RMP hyperpolarization (by 15.69 ± 2.42 mV; $t_{(27)}$ = 6.48, *** p < 0.0001, unpaired t-test; **C**), a reduction in the rate of spontaneous firing (by 1.32 ± 0.45 Hz; $t_{(27)}$ = 2.92, ** p = 0.007, unpaired t-test; **D**), a significant increase in rheobase levels (by 19.64 ± 4.38 pA; $t_{(26)}$ = 4.48, *** p = 0.0001, unpaired t-test; **E**), and an overall decrease in evoked firing frequency ($F_{(19,519)}$ = 25.4, *** p < 0.0001, two-way repeated measures ANOVA; **F**). **G.** Knockout of NALCN in spino-PB neurons resulted in an overall insensitivity of the RMP to Gd^{3+} application (n = 17 total, $F_{(1,30)}$ = 13.9, p = 0.0008, two-way ANOVA). Gd^{3+} application significantly hyperpolarized the RMP of GFP-infected neurons (by 8.29 ± 3.24 mV; n = 9 in each group, $t_{(30)}$ = 2.56, * p = 0.03, Holm-Sidak post-test; *left*), while having no significant effect on spino-PB projection neurons infected with Cre (n = 8 in each group, $t_{(30)}$ = 0.98, p = 0.33, Holm-Sidak post-test). **H.** Gd^{3+} application significantly increased rheobase in GFP-infected projection neurons (by 15 ± 5.46 pA; n = 9 in each group, $t_{(28)}$ = 2.7, * p = 0.02, two-way ANOVA, Holm-Sidak post-test; *left*) but not

in spino-PB neurons with NALCN knockout (0.71 ± 6.19 pA; n = 7 in each group, $t_{(28)}$ = 0.11, p = 0.33, Holm-Sidak post-test; *right*).

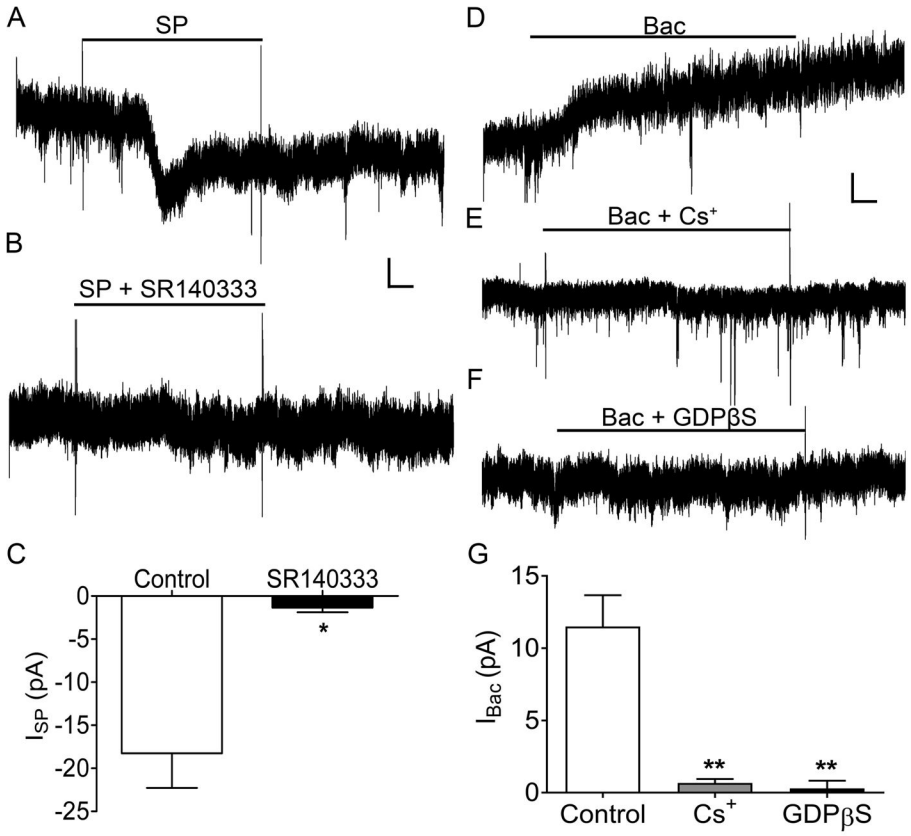

Figure 5. Strategy to explore the effects of Substance P (SP) on spinal projection neurons in the absence of GIRK activation

A. Representative current trace of I_{Hold} in response to 5 μM Substance P (SP; I_{SP}). Black line indicates the bath application of SP. **B.** Representative current trace of I_{Hold} in response to 5 μM SP, in the presence of the NK1R antagonist SR140333 (1 μM). Black line, bath application of SP in the presence of SR140333. Scale bars in **A, B**: 10 pA, 20 s. **C.** Transient inward I_{SP} is significantly reduced in the presence of SR140333 (by 16.9 ± 5.91 pA; SP: n = 6, SR140333: n = 3; $t_{(7)}$ = 2.86, * p = 0.024, unpaired t-test). **D – F.** Representative traces of outward currents evoked by the $GABA_BR$ agonist R-baclofen (100 μM; **D**) in identified spino-PB neurons in the presence of 100 μM extracellular Cs^+ (**E**) or 1 μM intracellular GDPβS (**F**). Scale bars in **D – F**: 10 pA, 20 s. G. The mean amplitude of baclofen-evoked current (I_{Bac}) was significantly reduced in the presence of Cs^+ or GDPβS (n = 3 in each group, $F_{(2,6)}$ = 23.9, p = 0.0014, one-way ANOVA). The application of Cs^+ significantly reduced I_{Bac} (by 10.83 ± 1.84 pA; $t_{(6)}$ = 5.89, ** p = 0.0018, Holm-Sidak post-test). Intracellular application of GDPβS also significantly decreased I_{Bac} (by 11.21 ± 1.84 pA; $t_{(6)}$ = 6.09, ** p = 0.0018, Holm-Sidak post-test).

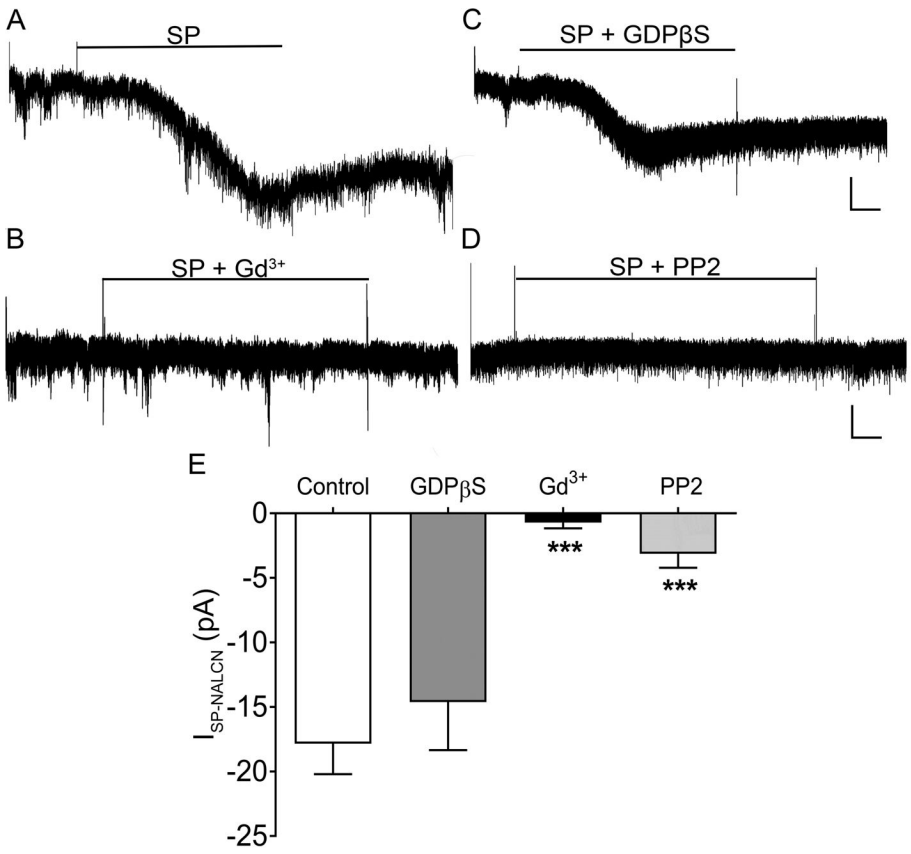

Figure 6. SP activates NALCN channels in rat spino-PB neurons via Src kinases

A – B. Under the experimental conditions detailed in Fig. 5, SP evoked a transient inward current (**A**; n = 9) that was blocked by Gd^{3+} (100 μM; n = 6; **B**), suggesting that the current was mediated by NALCN channels ($I_{SP\text{-}NALCN}$). **C – D**. $I_{SP\text{-}NALCN}$ was resistant to intracellular GDPβS (1 μM; n = 6; **C**), but was significantly reduced by the intracellular application of the Src kinase inhibitor PP2 (30 μM; n = 6; **D**). Scale bars in **A** and **C**: 10 pA, 20 s; **B** and **D**: 10 pA, 10 s. **E.** The amplitude of $I_{SP\text{-}NALCN}$ varied significantly in the presence of Gd^{3+}, GDPβS, and PP2 ($F_{(4,22)}$ = 9.85, p = 0.0001, one-way ANOVA). Gd^{3+} application significantly reduced $I_{SP\text{-}NALCN}$ compared to control measurements (by 17.13 ± 3.22 pA; Control: n = 9, Gd^{3+}: n = 6; $t_{(23)}$ = 5.32, *** p = 0.0001, Holm-Sidak post-test) while GDPβS administration did not significantly decrease $I_{SP\text{-}NALCN}$ when compared to controls (by 3.23 ± 3.22 pA; Control: n = 9, GDPβS: n = 6; $t_{(23)}$ = 1.002, p = 0.55, Holm-Sidak post-test). Meanwhile, PP2 significantly reduced $I_{SP\text{-}NALCN}$ compared to control measurements (by 14.71 ± 3.22 pA; Control: n = 9, PP2: n = 6; $t_{(23)}$ = 4.57, *** p = 0.0007, Holm-Sidak post-test).

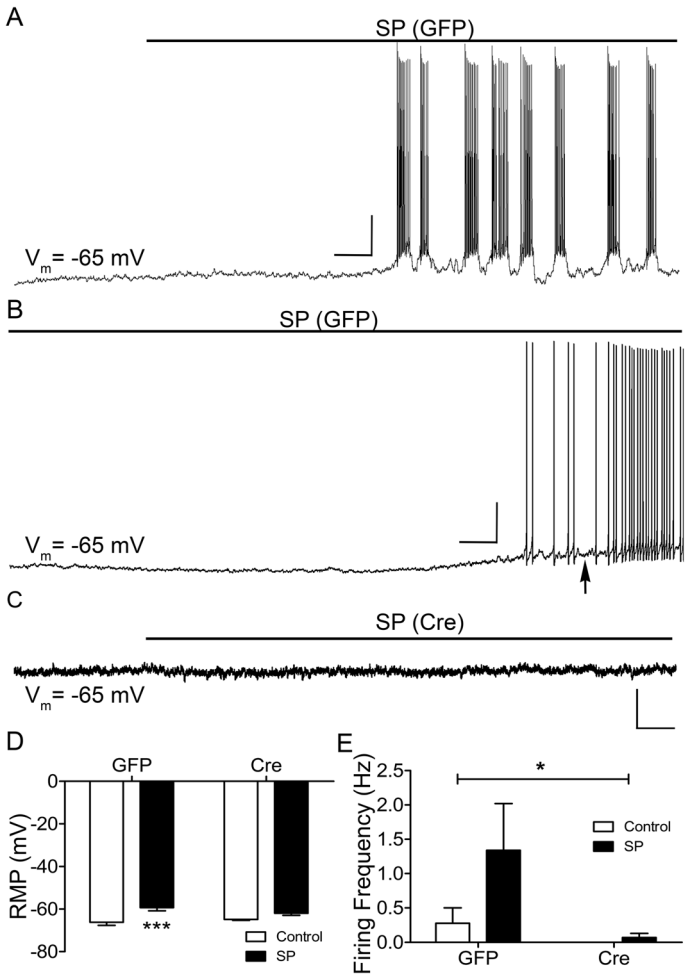

Figure 7. NALCN channel knockout significantly reduces substance P-evoked firing in spinal projection neurons

A – C. Representative traces of SP-evoked firing in identified GFP (**A, B**) and NALCN knockout (**C**) spino-PB neurons. RMP was maintained near −65 mV prior to SP application. Scale bars in **A**: 20 mV, 10 s; **B**: 20 mV, 5 s; **C**: 10 mV, 10 s. Black arrow indicates a representative region where RMP measurements were obtained during SP application. **D.** The effects of SP (5 μM) application on the RMP varied significantly between spino-PB neurons that were infected with GFP versus spino-PB neurons after NALCN knockout (n = 8 in each group, $F_{(1,28)} = 17.23$, p = 0.0003, two-way ANOVA). SP application significantly depolarized control GFP-expressing spino-PB neurons (by 6.90 ± 1.66 mV; $t_{(28)} = 4.16$, *** p = 0.0006, Holm-Sidak post-test) but had no significant effect on neurons with NALCN knockout (2.8 ± 1.66 mV; $t_{(28)} = 1.7$, p = 0.1, Holm-Sidak post-test). **E.** SP-evoked action potential generation was significantly greater in control GFP-expressing projection neurons versus NALCN knockout projection neurons (n = 8 in each group, $F_{(1,28)} = 4.62$, * p = 0.04, two-way ANOVA).